HHS Public Access

Author manuscript

Sci Transl Med. Author manuscript; available in PMC 2024 June 28.

Published in final edited form as:

Sci Transl Med. 2023 June 28; 15(702): eadd1175. doi:10.1126/scitranslmed.add1175.

Notch signaling drives intestinal graft-versus-host disease in mice and non-human primates

Victor Tkachev[1,2,†], **Ashley Vanderbeck**[3,4,†], **Eric Perkey**[3,5,†], **Scott N. Furlan**[6], **Connor McGuckin**[2], **Daniela Gómez Atria**[3,‡], **Ulrike Gerdemann**[2], **Xianliang Rui**[2], **Jennifer Lane**[2], **Daniel J. Hunt**[7], **Hengqi Zheng**[7], **Lucrezia Colonna**[7,‡], **Michelle Hoffman**[6], **Alison Yu**[7], **Riley Outen**[3], **Samantha Kelly**[3], **Anneka Allman**[3], **Ute Koch**[8], **Freddy Radtke**[8], **Burkhard Ludewig**[9], **Brandon Burbach**[10], **Yoji Shimizu**[10], **Angela Panoskaltsis-Mortari**[11], **Guoying Chen**[12], **Stephen M. Carpenter**[12,‡], **Olivier Harari**[12], **Frank Kuhnert**[12], **Gavin Thurston**[12], **Bruce R. Blazar**[11], **Leslie S. Kean**[2,†,*], **Ivan Maillard**[3,†,*]

[1]Massachusetts General Hospital, Center for Transplantation Sciences, Boston, MA 02114.

[2]Division of Hematology/Oncology, Boston Children's Hospital and Department of Pediatric Oncology, Dana Farber Cancer Institute, Department of Pediatrics, Harvard Medical School, Boston, MA 02115.

[3]Division of Hematology/Oncology, Department of Medicine, Perelman School of Medicine, University of Pennsylvania, Philadelphia, PA 19104.

[4]Immunology Graduate Group and Veterinary Medical Scientist Training Program, University of Pennsylvania, Philadelphia, PA 19104.

[5]Graduate Program in Cellular and Molecular Biology, University of Michigan, Ann Arbor, MI 48109.

[6]Clinical Research Division, Fred Hutchinson Cancer Research Center, University of Washington, Seattle, WA 98109.

[7]Ben Towne Center for Childhood Cancer Research, Seattle Children's Research Institute, University of Washington, Seattle, WA 98101.

[8]EPFL, 1015 Lausanne, Switzerland.

[*]co-corresponding authors: Leslie S. Kean, leslie.kean@childrens.harvard.edu Ivan Maillard, imaillar@pennmedicine.upenn.edu.
[†]These authors contributed equally to this work
[‡]Current affiliations – D.G.A.: Immunology Research Unit, GlaxoSmithKline, Collegeville, PA 19426; L.C.: Juno Therapeutics, Seattle, WA 98109; S.M.C.: Division of Infectious Diseases and HIV Medicine, Department of Medicine, Case Western Reserve University School of Medicine, Cleveland, OH 44106.

Author contributions: V.T., A.V., and E.P. designed all research studies, performed experiments and analyzed data. C.M., D.G.A, U.G., X.R., J.L., D.J.H., H.Z., L.C., M.H., A.Y., R.O., S.K., A.A., and G.C. performed experiments and analyzed data. V.T. and S.N.F. performed bioinformatic analysis. A.P-M. performed histopathological scoring. U.K., F.R., B.L., B.B., and Y.S. provided critical reagents and advice. S.M.C., O.H., F.K., G.T., and B.R.B. provided critical reagents or advice with experimental design and data interpretation. L.S.K. and I.M. selected the research questions and defined the overall experimental approach. V.T., L.S.K., and I.M. wrote the manuscript, and all authors reviewed it.

Supplementary Materials:
Supplementary Materials and Methods
Fig. S1 to S11
MDAR Reproducibility Checklist
Data Files S1 to S9

[9]Medical Research Center, Kantonsspital St. Gallen, 9007 St. Gallen, Switzerland.

[10]Department of Laboratory Medicine and Pathology, Center for Immunology, Masonic Cancer Center, University of Minnesota School of Medicine, Minneapolis, MN 55455.

[11]Division of Blood & Marrow Transplant & Cellular Therapy, Department of Pediatrics, University of Minnesota School of Medicine, Minneapolis, MN 55455.

[12]Regeneron Pharmaceuticals Inc., Tarrytown, NY 10591.

Abstract

Notch signaling promotes T cell pathogenicity and graft-versus-host disease (GVHD) after allogeneic hematopoietic cell transplantation (allo-HCT) in mice, with a dominant role for the Delta-like Notch ligand, DLL4. To assess if Notch's effects are evolutionarily conserved and to identify the mechanisms of Notch signaling inhibition, we studied antibody-mediated DLL4 blockade in a non-human primate (NHP) model similar to human allo-HCT. Short-term DLL4 blockade improved post-transplant survival with durable protection from gastrointestinal GVHD in particular. Unlike prior immunosuppressive strategies tested in the NHP GVHD model, anti-DLL4 interfered with a T cell transcriptional program associated with intestinal infiltration. In cross-species investigations, Notch inhibition decreased surface abundance of the gut-homing integrin α4β7 in conventional T cells while preserving α4β7 in regulatory T cells, with findings suggesting increased β1 competition for α4 binding in conventional T cells. Secondary lymphoid organ fibroblastic reticular cells emerged as the critical cellular source of Delta-like Notch ligands for Notch-mediated up-regulation of α4β7 integrin in T cells after allo-HCT. Altogether, DLL4-Notch blockade decreased effector T cell infiltration into the gut, with increased regulatory to conventional T cell ratios early after allo-HCT. Our results identify a conserved, biologically unique and targetable role of DLL4-Notch signaling in intestinal GVHD.

One Sentence Summary:

Evolutionarily conserved Notch signaling promotes pathogenic effector T cell infiltration of the intestine during acute graft-versus-host disease.

INTRODUCTION

Allogeneic hematopoietic cell transplantation (allo-HCT) has life-saving potential for patients with hematological malignancies and bone marrow disorders. However, acute graft-versus-host disease (aGVHD) remains a major cause of morbidity and mortality (1). Among aGVHD manifestations, gastrointestinal involvement (GI-aGVHD) is most challenging, with nearly all cases of severe aGVHD prominently involving the gastrointestinal tract. Moreover, epithelial injury and the gut microbiome can fuel activation of pathogenic T cells, thereby propagating tissue damage after allo-HCT (2–8). Thus, preventing GI-aGVHD would represent a major advance if accomplished while preserving protective immunity, including anti-infectious and anti-cancer T cell responses (9).

To foster progress, preclinical studies have relied heavily on mouse allo-HCT models. Major advantages include strain combinations that mimic many aspects of aGVHD, as

well as abundant genetic and immunological reagents (10). Yet, mouse models do not account for evolutionary changes in biological pathways driving aGVHD, especially for complex ligand-receptor systems with multiple family members. Moreover, mouse allo-HCT differs from human allo-HCT in terms of transplant conditioning, supportive care, and complications. Thus, numerous factors could underlie the failure of preclinical studies in mice to be translated to patients. To address these issues, we developed a T cell-replete haploidentical allo-HCT model of aGVHD in non-human primates (NHPs) (11–16). In this model, treatments can be evaluated initially as single agents for their activity in GVHD prophylaxis, unlike in human patients where new interventions must be combined with drugs used for routine GVHD prevention. Thus, the impact of targeting a single pathway can be studied in detail in NHP (12, 13, 15, 16). Among key parameters for subsequent translation, the NHP model can establish the magnitude of single agent activity, assess if the pathway of interest is conserved from mice to primates and thus worth targeting in humans, and detect unexpected toxicities not predicted in mice. Furthermore, the NHP model can identify unique mechanisms of GVHD protection to define how new strategies should best be deployed in humans.

We previously reported that early post-transplant Notch inhibition in donor T cells induced major protection from GVHD in mice (17–21). Notch is an evolutionarily conserved ligand-receptor signaling pathway. Mammals harbor four agonistic Notch ligands (Delta-like1/4, Jagged1/2) and four receptors (Notch1 to 4), with both redundant and non-redundant functions (22, 23). Ligand-receptor interactions lead to proteolytic cleavage of Notch receptors by γ-secretase, followed by translocation of intracellular Notch to the nucleus where it induces target gene activation in association with the transcription factor RBP-Jκ and a Mastermind-like family co-activator. In mouse allo-HCT models, genetic or pharmacologic Notch inhibition in donor T cells led to major protection from aGVHD, while preserving T cell expansion in lymphoid organs and potent graft-versus-tumor activity – a beneficial pattern of immunomodulation (17–21, 24–26). Notch1/2 in T cells and Delta-like1/4 (DLL1/4) in the host underlied the effects of Notch signaling on GVHD, with a dominant role for Notch1 and DLL4 (17, 21, 24). Donor T cells interacted with Delta-like ligands expressed by fibroblastic reticular cells in secondary lymphoid organs within hours of transplantation, consistent with an early window of pathogenic Notch activity (24). Indeed, Notch inhibition within two days of allo-HCT was essential to confer GVHD protection, and a single dose of antibodies blocking Delta-like ligands provided long-term GVHD protection when given at the time of transplantation (24). Thus, our findings in mice suggest that transient inhibition of Delta-like Notch ligands is an attractive strategy to prevent GVHD after allo-HCT without causing global immunosuppression.

Despite these promising findings, it remains unknown if the critical impact of Notch signaling on GVHD in mice will be conserved in humans. Although its overall effects are preserved between species, Notch is a complex pathway driven by multiple receptors and ligands whose individual involvement can drift through evolution. Furthermore, systemic Notch inhibitors such as γ-secretase inhibitors induced on-target toxicity in mice and in human clinical trials, especially when given continuously (21, 27–29). In contrast, targeting individual Notch ligands and receptors with blocking antibodies conferred a broader therapeutic window (21, 30). Thus, it is essential to define the overall activity, tolerability,

temporal effects and mechanisms-of-action of Notch pathway inhibitors in models of allo-HCT and GVHD as close to human allo-HCT as possible.

To address these questions, we turned to our haploidentical allo-HCT model in NHPs, which recapitulates key aspects of human allo-HCT, providing a translational platform for investigational drugs and mechanistic analysis. Using this approach, we previously nominated therapeutic strategies studied initially in mice as candidates for human translation (11–16), with the first (CTLA4-Ig) now FDA-approved for GVHD prevention (31). Given the dominant role of the Notch ligand DLL4 in mice, we prioritized transient peri-transplant DLL4 inhibition as the most promising strategy. We tested an anti-DLL4 antibody (REGN421) cross-reactive with human and NHP DLL4 for which pharmacokinetic and toxicity information was available from prior studies in NHPs and patients with cancer (32). In the NHP allo-HCT model, transient DLL4 inhibition with one dose or three weekly doses of REGN421 had potent single agent activity against clinical and pathologic GI-aGVHD, a pattern of activity not observed previously in NHP with other candidate therapeutics. Mechanistic analysis revealed decreased accumulation of activated conventional T cells in the GI tract and an increased ratio of regulatory to conventional T cells, both in NHPs and in mice. Notch-deprived effector, but not regulatory, T cells had decreased surface expression of the gut-homing integrin α4β7, which interacts with endothelial MAdCAM-1 close to intestinal crypts (5). Our data suggest a mechanism for decreased α4β7 through enhanced β1 and β7 competition for α4 binding upon Notch blockade. Together, we identified a conserved pathogenic role of the Notch ligand DLL4 from mice to NHP, with therapeutic benefits of transient DLL4 inhibition in preventing GI-aGVHD. Our data provide information about the unique effects of Notch inhibition on the differential accumulation of regulatory and conventional T cells in the gut. In turn, these observations provide insights into the development of Notch targeting strategies to prevent GVHD in patients who receive allo-HCT.

RESULTS

DLL4 blockade early after allo-HCT protects NHPs from GI-aGVHD.

Our prior experiments in mice demonstrated that short-term blockade of Delta-like Notch ligands starting within 2 days of allo-HCT had protective effects against aGVHD (21, 24). To evaluate if these effects translate to NHPs, we treated NHP allo-HCT recipients (all haplo-identical half-siblings) with the anti-DLL4 blocking antibody REGN421, using one of two dosing regimens: a single dose of 3 mg/kg at day 0 post-HCT (n=7), or three weekly doses at days 0, 7, and 14 (n=4). We then compared these NHP to allo-HCT recipients receiving supportive care only (“NoRx”) (Fig. 1A). Our NoRx cohort included half-siblings and unrelated haplo-identical recipients plus one unrelated major histocompatibility complex (MHC)-mismatched animal. However, we did not observe any differences between half-siblings and unrelated sub-cohorts in clinical or immunological aGVHD manifestations (fig. S1), providing the rationale to combine all untreated recipients into one single control cohort. Untreated and REGN421-treated recipients received comparable doses of T cells and $CD34^+$ cells (fig. S2A, data file S1). Pharmacokinetic analysis after a single dose of REGN421 demonstrated mono-phase decay kinetics with a half-life of 3.36 days, resulting

in biologically active serum concentrations >2 μg/mL (33) until day 17±2 days (fig. S2B). Three weekly doses of REGN421 resulted in antibody concentrations >2 μg/mL for >30 days post-HCT (fig. S2B).

Protection from aGVHD was observed with a single dose of REGN421 at day 0 or three weekly doses at day 0, 7, and 14, consistent with an impact of REGN421 during the early phases of T cell activation (Fig. 1B and C). REGN421-treated animals had delayed aGVHD onset and lengthened survival compared to controls with no prophylaxis (NoRx; Fig. 1B and C). Although euthanasia decisions in this and other studies were solely based on humane veterinary endpoints, this was consistent with our past data documenting an inverse correlation between GVHD severity and post-HCT survival in this model (11, 13, 15, 16).

Detailed analysis of aGVHD clinical presentations in REGN421-treated animals in comparison to NoRx controls revealed near complete protection from GI-aGVHD with REGN421. None of the eleven recipients that received either single or multiple doses of REGN421 developed clinical signs of GI-aGVHD (Fig. 1D). Moreover, pathology scores in the GI tract remained lower with REGN421 compared to the NoRx cohort and equivalent to scores in healthy non-transplanted NHP (Fig. 1E). However, REGN421-treated recipients did ultimately develop other clinical and pathologic signs of skin, hepatic or pulmonary aGVHD, but without GI disease (data file S1, Fig. 1D and E, fig. S2C). These observations are consistent with partial protection from aGVHD after DLL4 inhibition, but with complete protection from GI-aGVHD by clinical and pathological criteria.

NHPs receiving mono-prophylaxis with a single dose or three weekly doses of REGN421 had rapid donor engraftment after allo-HCT (fig. S2D to K), including high bone marrow, whole blood, as well as T cell donor chimerism (Fig. 1F, fig. S2D). Nine out of eleven recipients showed hematologic reconstitution post-transplant (Fig. 1G and H); two animals (R.306 and R.297, each treated with a single dose of REGN421) were euthanized early after transplant (on day +12 and +11, respectively, prior to neutrophil engraftment). R.306 exhibited pre-engraftment bleeding complications, and R.297 developed a pre-engraftment GI infection (data file S1), both of which are expected complications after allo-HCT in NHP (12) and patients (34, 35). We observed a similar frequency of clinical events resulting in early euthanasia before neutrophil engraftment and a similar incidence of bleeding events or transfusion-refractory thrombocytopenia in the anti-DLL4 cohort compared to previously reported cohorts with other single-agent immunoprophylaxis that had comparable post-transplant survival (sirolimus versus costimulatory blockade with anti-OX40 ligand [OX40L] or anti-CD28 antibodies) (12, 13) (fig. S2K to N). These observations suggest that REGN421-based GVHD prophylaxis did not cause unique hematological toxicity in NHPs. As our 1-dose and 3-dose anti-DLL4 cohorts were similar by clinical, pathological and immunological criteria, all data from these cohorts were merged in subsequent analyses. Together, our findings suggest that DLL4 blockade can be achieved after allo-HCT in NHPs without drug-associated toxicity, without interfering with donor engraftment, and with protective activity against GI-aGVHD.

DLL4 blockade preserves mature T cell differentiation and reconstitution despite preventing GI aGVHD.

Our group previously examined OX40L blockade with KY1005 (13) and CD28 blockade with FR104 (12) for their ability to prevent T cell activation and prolong aGVHD-free survival in NHPs. With these antibodies, aGVHD prevention correlated with a block in T cell activation and maturation, resulting in substantial relative increases of $CD4^+$ and $CD8^+$ T cells with a naïve phenotype (fig. S3A and B), although absolute numbers of naïve $CD4^+$ and $CD8^+$ T cells in recipients treated with KY1005 or FR104 (and REGN421) were similar (fig. S3C and D). In contrast, flow cytometric analysis showed that, despite protection from GI-aGVHD, REGN421 did not block T cell differentiation after HCT. Indeed, the expected pattern of post-transplant naïve-to-central-memory and effector-memory transitions in $CD4^+$ T cells, and naïve-to-effector-memory and terminal-effector transitions in $CD8^+$ T cells were similar in REGN421-treated animals and the NoRx cohort (Fig. 2A and B, fig. S3A and B). Although proportions of proliferating $Ki67^+CD4^+$ and $CD8^+$ T cells were reduced in REGN421-treated compared to NoRx animals (Fig. 2C), other activation markers were similar. This included equivalent upregulation of OX40 and programmed cell death protein 1 (PD-1) on blood $CD4^+$ T cells (Fig. 2D and E), and upregulation of CD69 on $CD8^+$ T cells in both cohorts, with a slightly delayed but preserved upregulation of PD-1 on $CD8^+$ T cells in the REGN421 cohort (Fig. 2D to F). Yet, DLL4 inhibition induced similarly prolonged survival after allo-HCT (median survival time [MST] = 22 days) compared with the KY1005 anti-OX40L (MST = 19.5 days) (13) and the FR104 anti-CD28 antibody (MST = 21 days) (12) (fig. S3E). Importantly, unlike REGN421, treatment with KY1005 or FR104 did not improve GI pathology compared with the NoRx GVHD cohort (fig. S3F). Together, these data suggest that Notch inhibition protects allo-HCT recipients from aGVHD by mechanisms other than those of OX40L- or CD28-directed costimulation blockade.

REGN421 prophylaxis decreases cell surface α4β7 integrin in $CD8^+$ T cells after allo-HCT.

Given that REGN421 specifically protected from GI-aGVHD, but not liver or skin aGVHD, we hypothesized that DLL4 blockade early after allo-HCT altered unique aspects of aGVHD pathogenesis, including migration of activated T cells to the GI tract. To test this hypothesis, we studied homing molecules controlling T cell migration into visceral organs during aGVHD (36–40). We analyzed relevant chemokine receptors and integrins using flow cytometry (CCR5, CCR9 and CXCR3, as well as the integrin α4β7) and quantified mRNA for the chemokine receptor gene *CXCR6* (37), for which rhesus macaque-reactive antibodies do not exist. REGN421 did not impact expression of CCR5, CXCR3, CXCR6, or CCR9 (fig. S4A to D), but decreased expression of the GI tract-homing integrin α4β7 on $CD8^+$ T cells in blood (Fig. 3A to D), spleen (Fig. 3E and F) and mesenteric lymph nodes (mLN; Fig. 3G and H) compared to NoRx controls. Decreased cell surface α4β7 correlated with fewer $\alpha4\beta7^+CD8^+$ T cells also expressing CCR9 in REGN421-treated compared to NoRx controls (fig. S4E). Further analysis revealed that DLL4 blockade decreased α4β7 expression in $CD8^+$ T cells with central-memory, effector-memory and effector phenotypes, whereas expression in naïve and stem cell-memory subsets was equivalent in NoRx and REGN421 cohorts (fig. S4F). These results suggest that DLL4 blockade affects surface α4β7 in T cells without affecting progression through T cell memory/effector differentiation. Importantly, whereas development of aGVHD in the NoRx cohort was associated with lower α4β7

expression in regulatory T cells (T_{reg} cells) compared to heathy controls, DLL4 blockade normalized the proportion of $\alpha4\beta7^+$ T_{reg} cells (Fig. 3G and H). Thus, REGN421 decreased cell surface α4β7 in conventional T (T_{conv}) cells while preserving it in T_{reg} cells.

To test if regulation of cell surface α4β7 in REGN421-treated animals correlated with T_{conv} and T_{reg} cell abundance in the GI tract compared to NoRx controls, we studied gut samples from transplant recipients. In the NoRx aGVHD cohort, we observed increased infiltration by activated $Ki67^+CD3^+$ T cells in the intestine at terminal analysis (Fig. 4A to C, fig. S4G) compared to healthy controls. DLL4 blockade decreased the abundance of $Ki67^+$ T cells (Fig. 4A to C, fig. S4G), which we previously identified as GI-aGVHD-associated tissue-infiltrating T cells (compared to non-infiltrating resident recipient-derived T cells that survived transplant conditioning and were largely $Ki67^-$) (11). At the same time, total numbers of $CD3^+$ T cells in the intestine were unchanged (fig. S4G). These data may reflect recent findings that, unlike in mice, large numbers of host-derived tissue-resident T cells can survive in barrier organs (including the colon) and persist long after myeloablative conditioning in humans and NHP (11, 41, 42), Thus, our results suggest progressive replacement of recipient tissue-resident T cells with activated $Ki67^+$ donor-derived T cells recruited into the inflamed colon.

In addition, REGN421 increased the T_{reg}:T_{conv} ratio and the percentage of $CD25^+CD127^-$ $FoxP3^+$ T_{reg} cells in the GI tract compared to the NoRx cohort (Fig. 4D and E). In the liver, however, the T_{reg}:T_{conv} ratio was similar in REGN421-treated and NoRx cohorts (Fig. 4D and E). The differential impact of REGN421 on T_{reg} and T_{conv} cell recruitment to the GI tract could be related to relatively preserved expression of α4β7 in T_{reg} cells after DLL4 blockade as compared to reduced cell surface α4β7 in T_{conv} cells (Fig. 3E to H).

In a mouse allo-HCT model, Notch inhibition blunts α4β7 upregulation and intestinal accumulation of conventional $CD4^+$ and $CD8^+$ T cells, but preserves intestinal T_{reg} cells.

To gain mechanistic information about T cell-intrinsic effects of Notch on cell surface α4β7 and gut homing, we used a lethally irradiated parent-to-F1 MHC-mismatched mouse model with a sublethal dose of T cells, blocking all Notch signals in donor $CD4^+$ and $CD8^+$ T cells through expression of the pan-Notch inhibitor DNMAML (*Cd4-Cre*$^+$*ROSA*^{DNMAML} mice) (19, 21) (Fig. 5, fig. S5). *Cd4-Cre*^{neg} or *Cd4-Cre*$^+$*ROSA*^{WT} mice were used as controls (fig. S6). These experiments enabled a detailed kinetic analysis of α4β7 expression and T cell homing to the gut that was not possible in NHPs. DNMAML expression in T cells prevented both weight loss and thymic injury, two representative features of aGVHD (fig. S5A and B). As reported previously (19, 21, 24), Notch inhibition led to an increased proportion of T_{reg} cells at multiple sites in allo-HCT recipients (fig. S5C and D). Next, we quantified cell surface α4β7 in activated donor-derived T cells at day 4, 7, 14, and 28 after transplant. At day 4, DNMAML blunted the induction of cell surface α4β7 in $CD8^+$ and in $Foxp3^-CD4^+$ T_{conv} cells in spleen and mLN (Fig. 5B and C). In contrast, $Foxp3^+CD4^+$ DNMAML T_{reg} cells had preserved or even increased α4β7 on their surface. The impact of Notch inhibition on α4β7 persisted at later time points in $CD8^+$, but not $CD4^+$ T cells, similarly to findings in NHP and showing evolutionary conservation (Fig. 5B and C, Fig. 3).

Because Notch inhibition had divergent effects on α4β7 in T_{conv} versus T_{reg} cells that could differentially affect homing to the GI tract, we designed a competitive assay for the accumulation of wild-type and Notch-deprived DNMAML T cell subsets in recipient organs (Fig. 5D). We injected a 1:1 mixture of wild-type and DNMAML T cells into irradiated allo-HCT recipients versus DNMAML T cells alone as a control. We tracked the percentage of Notch-deprived T cells in secondary lymphoid organs and GVHD target organs based on expression of the DNMAML-GFP fusion protein in donor-derived $CD44^+$ T cells (Fig. 5E and F). In the spleen, mLN, and liver, we recovered a ratio of wild-type to DNMAML T_{conv} cells close to the 1:1 ratio in the inoculum, both for $CD8^+$ and $Foxp3^-CD4^+$ T_{conv} cells. In contrast, the colon (Fig. 5E and F) and small intestine (Fig. 5F) contained decreased proportions of DNMAML-GFP^+CD8^+ and $Foxp3^-CD4^+$ T cells, consistent with cell-autonomous effects of Notch inhibition on their accumulation in the gut. For $Foxp3^+CD4^+$ T_{reg} cells, we observed expansion of DNMAML-GFP^+ T_{reg} cells in secondary lymphoid organs, and preservation of DNMAML T_{reg} cell accumulation in the gut (as evidenced by a lower wild-type to DNMAML ratio among T_{reg} cells compared to T_{conv} cells) (Fig. 5E and F). Similar findings were apparent with a 1:2 wild-type to DNMAML T cell inoculum (fig. S5E). Using the same design, we confirmed that DNMAML-mediated Notch inhibition decreased cell surface α4β7 through cell-autonomous mechanisms (Fig. 5G, fig. S5F and G). Thus, Notch signals increase α4β7 abundance and gut-homing potential in alloreactive T_{conv} cells, but not in T_{reg} cells. Altogether, complementary NHP and mouse data suggest that Notch inhibition blunts intestinal homing of T_{conv} cells, while preserving that of T_{reg} cells, leading to increased T_{reg}:T_{conv} ratios in the GI tract early after transplantation.

We then compared the impact of pan-Notch inhibition in T cells with DNMAML to systemic DLL4 blockade in mice (fig. S7). To accomplish this, we obtained a mouse-specific anti-DLL4 antibody (REGN577), as REGN421 blocks primate but not mouse DLL4. REGN577 administration or DNMAML expression in T cells decreased α4β7 integrin in donor-derived $CD8^+$ and $Foxp3^-CD4^+$ T_{conv} cells, although the magnitude of these effects was higher with DNMAML than REGN577 (fig. S7A and B). This was also apparent by detection of the α4β7 heterodimer (fig. S7C and D). Similarly, both REGN577 and DNMAML increased the proportion of donor-derived T cells expressing both α4 and β1, while decreasing the proportion of $\alpha4^+\beta1^-$ T cells (fig. S7E and F). These findings indicate similar effects of both interventions on integrin expression in alloreactive T cells, although the difference in effect size suggests a contribution of other Notch ligands besides DLL4. This is consistent with our past work using other endpoints documenting the contribution of DLL1 and DLL4 Notch ligands to GVHD pathogenesis in mice (21, 24), with a dominant role for DLL4 and more minor contributions of DLL1.

Fibroblastic reticular cells are the critical source of Delta-like Notch ligands driving α4β7 expression and gut-homing potential in alloreactive T cells.

We previously showed that Notch ligands expressed by secondary lymphoid organ *Ccl19-Cre*$^+$ fibroblastic reticular cells (FRCs) interact with Notch receptors in donor T cells at early stages after transplantation to drive GVHD pathogenesis (24, 25). Indeed, *Ccl19-Cre*-mediated *Dll1* and *Dll4* Notch ligand gene inactivation in recipient FRCs increased

survival after allo-HCT and improved clinical GVHD scores to a similar extent as pan-Notch inhibition in donor T cells (24, 25). To assess if stromal Notch ligands also drive changes in gut-homing molecules and gut-homing potential of allo-T cells, we performed allo-HCT in *Ccl19-Cre;Dll1*$^{f/f}$*;Dll4*$^{f/f}$ CBF1 mice (Fig. 6A) (24, 43). Stroma-specific *Dll1/4* inactivation with *Ccl19-Cre* decreased α4β7 expression among donor-derived T cells (Fig. 6B and C) as well as T cell infiltration into the gut (Fig. 6D and E) to a similar extent as observed with other methods of Notch inhibition. Thus, early T cell exposure to Delta-like Notch ligands in lymphoid tissue fibroblastic niches is critical to induce the Notch-dependent gut-homing program in alloreactive T cells.

DLL4 blockade induces complex changes in the T cell transcriptome and is associated with normalization of an aGVHD-specific T cell GI-infiltration signature.

To gain insights into how Notch inhibition affects T cells after allo-HCT, we explored transcriptomic changes using Rhesus macaque-specific gene arrays (12, 13, 15, 16) (data file S2). T cells were purified from blood on day 15 after HCT ('REGN421.D15' group) and at necropsy ('REGN421.Nx' group). Transcriptomes were compared to three other datasets: (1) the NoRx aGVHD cohort, with gene arrays obtained at necropsy (MST=8 days, n=12); (2) recipients treated with the KY1005 anti-OX40L antibody (MST=19.5 days, blood for gene arrays at day 15, n=4) (13); (3) recipients treated with the FR104 anti-CD28 (MST=26 days, blood for gene arrays at day 15, n=3) (12). Importantly, neither OX40L nor CD28 blockade offered specific protection from clinical GI-aGVHD, and pathological scores at terminal analysis were not different in KY1005, FR104, and NoRx aGVHD cohorts (fig. S3F).

We next sought to identify a T cell transcriptomic signature associated with inhibition of GI infiltration after DLL4 blockade. Compared to NoRx aGVHD controls, blood T cells from REGN421-treated animals at day 15 and at necropsy demonstrated decreased enrichment for an aGVHD-specific GI infiltration signature recently discovered by our group (11), which includes multiple chemotaxis-related genes. In contrast, this signature was enriched in the NoRx versus healthy control cohort (fig. S8A). Neither anti-OX40L nor anti-CD28-prophylaxed cohorts normalized the T cell GI infiltration signature (fig. S8A), suggesting that these interventions had effects distinct from those of DLL4 blockade.

To better understand REGN421-specific mechanisms of aGVHD protection, we identified differentially expressed genes that were exclusive to the comparison of REGN421 versus NoRx, and not found when comparing anti-OX40L or anti-CD28 to NoRx (fig. S8B, data file S2 to S4). We identified 357 overrepresented and 97 underrepresented transcripts specific to the REGN421 versus NoRx comparison. We identified only 61 overrepresented and 34 underrepresented shared transcripts among all three interventions compared to NoRx (fig. S8B, data file S3 and S4). Functional annotation and pathway analysis performed using Metascape (44) revealed that the shared GVHD protection signature predominantly involved cell cycle/DNA replication as well as cytokine signaling pathways (fig. S8C, data file S5). The REGN421-specific GVHD-protection signature was enriched in cell-cell communication and chemotaxis-related genes (fig. S8D and E, data file S6).

DLL4 blockade increases expression of the integrin β1 subunit while decreasing integrin β7 on the T cell surface.

We then investigated how Notch inhibition affects cell surface abundance of the α4β7 gut-homing integrin after allo-HCT in NHP T cells. *ITGA4* and *ITGB7* transcripts (encoding α4β7 subunits) were not decreased by DLL4 blockade with REGN421 (Fig. 7A). Thus, a simple transcriptional effect did not account for decreased α4β7 in T cells from REGN421-treated recipients. In contrast, *ITGB1* mRNA was increased in T cells from the REGN421 cohort (Fig. 7A). *ITGB1* encodes integrin β1, which interacts with α4 integrin and was reported to compete with β7 for α4 binding (45). To further investigate upregulated *ITGB1* expression in the REGN421 versus NoRx cohorts, ingenuity pathway analysis was utilized to identify putative upstream regulators. We found 22 upstream signaling molecules or pathways activated by REGN421, of which 9 included *ITGB1* as a target gene (fig. S8F, data file S7).

We next evaluated surface abundance of β1, β7 and α4 integrin chains. Consistent with mRNA, cell surface β1 expression was increased in $CD8^+$ T cells from REGN421-treated versus NoRx animals (fig. S8G and H). In contrast, surface β7 integrin was decreased (fig. S8G and H), despite comparable *ITGB7* transcripts in both cohorts (Fig. 7A). When assessing cell surface α4 and β1 together, we observed an increased proportion of $\alpha4^+\beta1^+CD8^+$ T cells and a decreased proportion of $\alpha4^+\beta1^-$ T cells in REGN421-treated as compared to NoRx recipients (Fig. 7B and C). These data are consistent with inhibition of β7 integrin trafficking to the cell surface by competitive binding of α4 by β1 (45, 46). Cell surface α4β7 is also regulated by availability of α4 integrin (47). However, *ITGA4* mRNA was similar in T cells from REGN421-treated and NoRx cohorts (Fig. 7A) and the proportion of $\alpha4^+CD8^+$ T cells was actually increased in the REGN421 cohort (fig. S8G and H). Thus, we hypothesize that DLL4 blockade results in upregulated expression of the integrin β1 subunit, leading to increased competition for α4 binding and decreased abundance of the α4β7 heterodimer.

Loss of integrin β1 rescues α4β7 expression in Notch-deprived alloreactive T cells.

To test if β1/β7 integrin subunit competition accounted for the effects of Notch inhibition on cell surface α4β7 in T cells, we used a mouse allo-HCT model with genetic inactivation of *Itgb1* and Notch signaling in T cells (*Cd4-Cre;Itgb1*$^{f/f}$*;ROSA*^{DNMAML} mice and respective controls). We lethally irradiated CBF1 recipients ($H\text{-}2^{b/d}$) and transplanted them with allogeneic T cell-depleted bone marrow plus T cells from *Cd4-Cre;ROSA*^{DNMAML}, *Cd4-Cre;Itgb1*$^{f/f}$, *Cd4-Cre;ROSA*^{DNMAML}*;Itgb1*$^{f/f}$ or wild-type littermate controls (all $H\text{-}2^{b}$). In activated donor-derived $CD44^{hi}CD8^+$ T cells, pan-Notch inhibition with DNMAML increased the proportion of T cells co-expressing α4 and β1, and decreased that of $\alpha4^+\beta1^-$ T cells (Fig. 7C). Donor-derived $CD4^+$ T cells showed similar findings (Fig. 7D, fig. S9A and B). The proportion of cells co-expressing cell surface α4 and β7 was lower among $\alpha4^+\beta1^+$ than $\alpha4^+\beta1^-$ T cells, consistent with β1/β7 competition for α4 binding (Fig. 7E). In activated donor $CD44^{hi}CD8^+$ T cells, pan-Notch inhibition with DNMAML decreased cell surface co-expression of α4 and β7 integrin subunits, and this effect was fully rescued by *Itgb1* inactivation (Fig. 7F). The same was true in donor-derived $Foxp3^-CD4^+$ T_{conv} cells (Fig. 7G, fig. S9C and D). In contrast, Notch inhibition did not decrease surface α4β7 in

T_{reg} cells, and even increased it in the absence of *Itgb1* (Fig. 7G, fig. S9C and D). To further corroborate these findings, we used an antibody specific for the α4β7 heterodimer. DNMAML decreased α4β7/LPAM-1 reactivity in $CD8^+$ T cells at day 4.5 and 14 after allo-HCT, and this effect was rescued by *Itgb1* inactivation (fig. S9E and F). More subtle effects of Notch inhibition on α4β7 were also apparent in *Itgb1*-deficient $CD4^+$ T cells, although in a different biological direction (with DNMAML increasing α4β7 in an *Itgb1*-independent manner) (fig. S8G, fig. S9D). Thus, the major effect of Notch inhibition to decrease α4β7 expression proceeds through *Itgb1*-dependent mechanisms.

We then asked whether *Itgb1*-dependent effects of Notch inhibition in T cells were cell-autonomous. To this end, we co-transplanted wild-type and DNMAML T cells with or without *Itgb1* expression into allogeneic recipients (Fig. 7H and I, fig. S9G and H). As assessed by detection of α4 and β7 subunits as well as α4β7/LPAM-1 reactivity, DNMAML markedly decreased the proportion of T cells with cell surface α4β7 integrin heterodimers through cell-autonomous mechanisms. This effect remained dependent on *Itgb1* expression in T_{conv} cells. Finally, we studied β1 abundance among different T cells subsets after allo-HCT (fig. S10). β1 expression was highest and most upregulated by Notch inhibition in $CD8^+$ T cells (followed by $CD4^+$ T_{conv} cells). In T_{reg} cells, overall β1 abundance was low, even upon Notch inhibition. Thus, cell-type specific differences in β1 expression could account for differential competition of β1 and β7 for α4 binding, with competition seen mostly in $\beta1^{hi}CD8^+$ T cells and, to a lesser extent, in $CD4^+$ T_{conv} cells. Altogether, Notch inhibition blunted cell surface α4β7 in an *Itgb1*-dependent manner in $CD4^+$ and $CD8^+$ T_{conv} cells after allo-HCT. In contrast, expression of this critical gut-homing integrin on the cell surface was preserved in Notch-deprived T_{reg} cells (fig. S11). These effects of Notch inhibition on the T cell gut-homing program occurred early after allo-HCT, within the critical time frame of initial gut seeding by alloreactive T cells.

DISCUSSION

Our observations uncover an impact of Notch signaling in the pathogenesis of GI-aGVHD, a major life-threatening complication of allo-HCT. Complementary investigations in mouse and NHP models demonstrated dominant effects of the Notch ligand DLL4 in GVHD that were conserved through evolution and could be targeted therapeutically. Furthermore, DLL4/Notch inhibition protected mice and NHPs from GI-aGVHD through unique mechanisms that differed from those of other, more global inhibitors of T cell activation (12, 13). This mechanism included normalization of a transcriptional T cell gut-homing signature recently discovered in the NHP aGVHD model (11). Decreased cell surface abundance of the α4β7 gut-homing integrin was a prominent and conserved effect of DLL4/Notch inhibition in effector T cells, whereas its expression was maintained in T_{reg} cells. Altogether, these findings highlight therapeutic opportunities and provide insights into evolutionarily conserved mechanisms of GI infiltration and GVHD pathogenesis that are predicted to also operate in patients.

First discovered in Drosophila, Notch signaling operates as a ligand/receptor system through conserved biochemical mechanisms (23). Mammals harbor multiple Notch ligands and receptors that are deployed in specific contexts, and whose relative importance can drift

between species (22, 48, 49). Thus, observations in mice should not be assumed to apply strictly to humans, even if the Notch pathway as a whole exerts conserved biological functions. This limitation is important for translational investigations, as it is not typically addressed by preclinical work in small animal models. In contrast, our findings in mice and NHPs document conserved effects of the Notch ligand DLL4 on T cell infiltration into the GI tract and GI aGVHD pathogenesis, with high single agent activity of DLL4 inhibitors. DLL4 is one of four agonistic Notch ligands in mammals, together with DLL1 and Jagged1/2 family ligands. We previously reported a critical role for Delta-like ligands in multiple mouse models of GVHD, with a dominant role for DLL4 and a more minor role for DLL1 (18, 19, 21, 24, 25). Our data indicate that the unique immunological functions of DLL4 in GVHD are conserved. The relative additional importance of DLL1 in NHPs will require further investigation. Furthermore, our findings support a role for Notch ligands of the Delta-like but not Jagged family in immune regulation.

Beyond the conserved role of DLL4 among other Notch ligands, key immunological effects of the Notch pathway in aGVHD were conserved through evolution. Both in mice and in NHP, DLL4/Notch inhibition did not protect from GVHD through global immunosuppression. Analysis of T cell reconstitution in REGN421-treated recipients showed expansion of donor-derived T cells with central-memory and effector-memory phenotypes, whereas naïve T cells were depleted, suggesting preserved alloantigen-mediated T cell activation and differentiation (50, 51). In contrast, anti-CD28 and anti-OX40L blunted in vivo T cell activation after allo-HCT in NHPs (12, 13), an effect also observed in clinical transplantation (31) that may lead to more global immune suppression. All REGN421-treated recipients were euthanized well before thymus-driven T cell reconstitution typically occurs in allo-HCT recipients, a process similarly protracted after NHP and human allo-HCT. Thus, the relative reduction of T cells with a naïve phenotype early post-HCT in REGN421-treated groups suggested their maturation to more differentiated subsets rather than defective thymic production of naïve T cells. In mice, we reported preserved in vivo expansion and differentiation of Notch-deprived alloreactive T cells in secondary lymphoid organs despite profound protection from aGVHD (18, 19, 21). Importantly, Notch inhibition in mice preserved efficient graft-versus-tumor (GVT) effects (19, 21). Although GVT activity cannot be studied directly with existing NHP models, our findings predict that DLL4/Notch blockade should preserve beneficial systemic anti-infectious and anti-cancer T cell immune responses after allo-HCT, which is highly desirable in patients. In addition, a short duration of DLL4/Notch blockade conferred protection from aGVHD, with all benefits derived from a single dose of antibodies at time of transplantation. Thus, any subsequent effects of the Notch pathway in T cell immunity, including de novo production of T cells in the thymus, should be restored after clearance of the blocking antibodies.

Instead of global immunosuppression, DLL4/Notch inhibition provided specific protection from GI-aGVHD, an effect not observed with other single agents tested for aGVHD prevention in NHPs. Indeed, protection from GI-GVHD emerged as the most conserved feature of DLL4/Notch blockade in mice and NHPs, although we have reported additional effects in mice. These observations highlight the strength of the NHP model to detect key new patterns of GVHD protection relevant to human allo-HCT. The NHP model, coupled to mechanistic investigations only possible in mice, provided unique insights into conserved

mechanisms of T cell infiltration into the GI tract after allo-HCT. Our findings suggest that rapid exposure of donor T cells to Notch ligands in secondary lymphoid organs within days after allo-HCT induces a gut-homing program that promotes early seeding of the gut by alloreactive T cells. The α4β7 integrin dimer was previously reported to play an important role in T cell migration and infiltration into the gut and in the pathogenesis of intestinal GVHD in mice (36, 52). α4β7 interacts with its ligand, MAdCAM1, expressed by endothelial cells in the intestinal lamina propria and in gut-associated lymphoid tissues (53, 54). Hanash and collaborators reported a critical role for this interaction in T cell recruitment to a vulnerable compartment containing intestinal stem cells at the base of intestinal crypts, with early injury to these cells playing a critical role in propagating GVHD (5). Both in mice and in NHPs, DLL4/Notch inhibition decreased cell surface α4β7 in conventional effector T cells. Mechanistically, these effects were not related to transcriptional regulation of *Itga4* or *Itgb7* expression by Notch, but instead to upregulated expression of *Itgb1* encoding the integrin subunit β1. Through this mechanism, β1 appeared to compete with β7 for α4 binding, as reported in other contexts (45). Although other mechanisms remain possible, the presence of *Itgb1* was necessary for Notch inhibition to decrease cell surface α4β7 in T cells after mouse allo-HCT. Importantly, upregulated *Itgb1* expression was detected in Notch-deprived NHP T cells together with normalization of a unique T cell gut-homing signature previously identified in NHPs through unbiased transcriptomic analysis (11). Thus, Notch emerges as a central regulator of T cell recruitment to the gut after allo-HCT, and Notch inhibitors exert beneficial effects in GVHD through effects that other interventions do not recapitulate.

Our findings in mice identify a specialized stromal cell niche in secondary lymphoid organs that upregulates α4β7 expression in alloreactive T cells through Notch ligand-dependent mechanisms early after allo-HCT. Retinoic acid (RA) production by retinal dehydrogenase enzymes (RALDH1–3) was also reported to induce α4β7 expression in T cells through separate mechanisms, with an important role for dendritic cells in gut-associated lymphoid tissues as a source of RA (55). However, non-hematopoietic stromal cells purified from mLNs also had high RALDH1–3 expression and could induce T cell α4β7 expression in culture and in ectopically transplanted LNs (56). Thus, stromal Notch ligands might cooperate with RA-dependent signals from dendritic cells and non-hematopoietic sources to induce α4β7 expression and other elements of the T cell gut-homing program after allo-HCT.

As a unique feature of DLL4/Notch inhibition in mice and NHP, cell surface α4β7 decreased in $CD4^+$ and $CD8^+$ T_{conv} cells early after allo-HCT while being maintained or even slightly increased in T_{reg} cells. In addition, Notch inhibition decreased the accumulation of T_{conv} cells in the gut while preserving T_{reg} cell recruitment, resulting in increased T_{reg}:T_{conv} ratios. This effect may be essential in shifting the early balance of T cells in the gut, creating a microenvironment with local immunosuppressive properties that blocks initiation of intestinal GVHD. Therapeutically, pan-inhibition of α4β7 is being explored in GVHD with the antibody vedolizumab (57, 58). A limitation of this intervention is to inhibit α4β7 equally in T_{conv} and T_{reg} cells. In contrast, the differential effects of DLL4/Notch inhibition in T_{conv} and T_{reg} cells may preserve T_{reg} cell recruitment, tilting the local ratio of pathogenic and protective T cells at a crucial stage in which the GI tract is

seeded by T cells after allo-HCT. DLL4/Notch inhibition may also exert protective effects independent of α4β7 regulation as part of its broader impact on the T cell gut homing signature that we identified.

Our work provides important new information about safety indicators of DLL4 inhibitors in a model closely recapitulating human allo-HCT. This is essential, given that the complex peri-transplant environment is not replicated in mice. Understanding the safety profile of REGN421 prophylaxis is even more important since, in allo-HCT, administration of Notch inhibitors coincides with a period of recovery from pre-transplant conditioning, a time of heightened clinical risk for patients. Reassuringly, short-term systemic DLL4 blockade with REGN421 did not trigger unexpected side effects in our NHP model, while preserving rapid engraftment as well hematopoietic and immune reconstitution. This is important, since unlike DLL4 blockade, pan-Notch inhibition with γ-secretase inhibitors or other non-selective approaches were poorly tolerated after allo-HCT in mice due to Notch inhibition in intestinal crypts (21). This intestinal toxicity is avoided by selective DLL4 blockade alone, which is not sufficient to trigger defects in intestinal homeostasis (21, 59). Furthermore, a single dose of REGN421 was sufficient to confer protection from GI-aGVHD, thus avoiding concerns about long-term DLL4 blockade which was reported to cause cardiovascular side effects after months of cumulative inhibition (29).

Limitations of the current study include the inability to thoroughly assess the long-term outcomes of DLL4 blockade in NHP, due to limitations in supportive care that curtail the duration of observation in this model. As Notch-deprived donor T cells demonstrated increased expression of α4β1 integrin, which could play a role in T lymphocyte trafficking to individual target tissues during GVHD, it is possible that DLL4 blockade may increase the risk of late-onset GVHD (even if not observed in mice or NHPs). Therefore, more studies, including using combinations of DLL4 antagonist(s) with other GVHD prophylactic interventions are warranted in clinically-relevant settings. Furthermore, a technical limitation of our studies in NHPs was the lack of time-matched analysis of target organs, such as colon, as all pathologic investigations were performed at terminal study endpoints that differed between experimental cohorts. This limitation was overcome in part by parallel experiments in mice enabling time-matched analysis. Finally, the lack of suitable reagents has thus far prevented us from investigating the contribution of DLL1 Notch ligands to GVHD pathogenesis in NHPs. Although DLL4 was dominant in mice and was thus selected as the focus of our NHP study, as well as a candidate therapeutic target, more work is needed to establish the impact of blocking DLL1, DLL4 or both ligands after allo-HCT.

Altogether, our data provide translational insights into the role of Notch signaling in T cell pathogenesis during aGVHD, with complementary input from observations in mice and NHPs. We reveal a central role for Notch signaling in the selective regulation of T cell homing and retention in the gut, with a differential impact on T_{conv} as opposed to T_{reg} cells. Practically, the unique single agent activity of REGN421 in NHP nominates DLL4 blockade as a worthwhile strategy to develop for the prevention of GI-aGVHD in patients, especially since it is predicted to have activity on a pathogenic gut homing program that other interventions do not neutralize. Possible future strategies include combination of DLL4 inhibitors with other agents to blunt aGVHD at non-intestinal sites. Alternatively, it would

be attractive to deploy DLL4 blockade in transplantation protocols in which GI involvement is the dominant manifestation of aGVHD. In addition, it will be interesting to investigate if DLL4/Notch signaling exerts conserved effects on immune cell homing and retention to target organs in other immunological contexts, such as intestinal autoimmune disorders.

MATERIALS AND METHODS

Study Design

Healthy, immunologically naïve juvenile and adult (mean age 5.9 years, range 2.1–14.8) Indian Rhesus macaques (*Macaca Mulatta*) of both sexes were obtained from breeding colonies at Alphagenesis Inc., UC Davis National Primate Research Center or Washington National Primate Research Center (WNPRC), and were housed at WNPRC or at Biomere Biomedical Research Models (BBRM). The study was conducted in accordance with USDA regulations and NIH recommendations in the Guide for the Care and Use of Laboratory Animals and was approved by the BBRM and the University of Washington/WNPRC Institutional Animal Care and Use Committees. This was a prospective study in NHPs designed to determine the biological role of Notch signaling in T cells during aGVHD, and the therapeutic effect of inhibiting Notch signaling by blocking Delta-like ligand 4 (DLL4). Several cohorts of transplant recipients were studied: (1) Allogeneic transplants with no GVHD prophylaxis (abbreviated ‘NoRx’, n = 11); (2) Allogeneic transplants receiving one dose of anti-DLL4 blocking antibodies from Regeneron (abbreviated ‘REGN421’, n = 7); and (3) Allogeneic transplants receiving three doses of REGN421 antibodies (n = 4). Cohort sizes were determined by taking into account the minimal number of animals needed to reach statistical significance, according to the ethical and IACUC mandate of “Replacement, Reduction, and Refinement” (60). Animal demographic parameters, transplant characteristics, and REGN421 doses administered in vivo are shown in data file S1. Allogeneic HCT, clinical and immunological monitoring, including longitudinal assessment of aGVHD clinical scores, were performed using our previously described strategy (13–16). For mouse transplantation, C57BL/6 × BALB/c F1 (CBF1, H-$2^{b/d}$) recipient mice were irradiated using a Cesium-137 source (11 Gy, two 5.5 Gy doses separated by 3 hours). Recipients were 8 to 16 weeks old. Female and male mice were used as recipients and equally distributed among groups. T cell-depleted bone marrow prepared with anti-Thy1.2 antibodies and complement (Cedar Lane Laboratories) was injected intravenously with or without B6 (H-$2^{b/b}$) wild-type T cells or T cells expressing the pan-Notch inhibitor DNMAML purified by EasySep negative magnetic selection (Stem Cell Technologies), as described (21). In selected experiments, donor wild-type and DNMAML T cells also lacked *Itgb1* expression. As an alternative to DNMAML-mediated Notch blockade, DLL4 was inhibited systemically using REGN577, a monoclonal antibody blocking mouse DLL4 (10 mg/kg i.p.). In selected experiments, suspensions of splenocytes and lymph node cells were transplanted without T cell purification.

Statistical analysis

All data were analyzed using Prism 9 (GraphPad). Survival data were analyzed using log-rank (Mantel-Cox) test. Flow cytometry data, immunofluorescent imaging data, and histological data were analyzed using one-way or two-way ANOVA with Tukey post-

hoc multiple comparison test, or Kruskal-Wallis tests, where appropriate. Technical and biological replicates are indicated in the figure legends. Error bars on the plots represent standard error of the mean (SEM). $p < 0.05$ was considered as significant. Sample size for in vivo experiments were determined on the basis of prior experience of effect sizes and variation to calculate power ("pwr" statistical package in R). Details of statistical methods used for each analysis are provided in figure legends. Details of the statistical analysis of gene array data are provided in the corresponding section.

Supplementary Material

Refer to Web version on PubMed Central for supplementary material.

Acknowledgments:

Funding:

This work was supported by the following sources: a Translational Research Program grant from the Leukemia and Lymphoma Society TRP-6583-20 (to L.S.K. and I.M.), National Institutes of Health R01-HL095791 (to L.S.K.), National Institutes of Health P01-HL158504 (to L.S.K.), National Institutes of Health U19-AI051731 (to L.S.K.), National Institutes of Health R01-AI091627 (to I.M.), National Institutes of Health R37-AI34495 (to B.R.B.), National Institutes of Health R01-HL56067 (to B.R.B.), National Institutes of Health R01-HL11879 (to B.R.B.), National Institutes of Health R01-HL-115114 (to B.R.B.), research funding from Regeneron, Inc., Be the Match Foundation/CIBMTR Amy Strelzer Manasevit Research Grant (to V.T.), ASTCT New Investigator Award (to V.T.), National Institutes of Health T32-AI070077 (to A.V.), National Institutes of Health T32-GM007863 (to E.P.), National Institutes of Health F30-AI161873 (to A.V.), and National Institutes of Health F30-AI136325 (to E.P.).

Competing interests:

D.G.A. is currently employed by GlaxoSmithKline. G.C., O.H., F.K., and G.T. are employed by Regeneron, and S.C. is a former employee. B.R.B. has received remuneration as an advisor to Magenta Therapeutics and BlueRock Therapeutics; research funding from BlueRock Therapeutics, Rheos Medicines, Carisma Therapeutics, Inc., and is a co-founder of Tmunity Therapeutics. L.S.K. is on the scientific advisory board for Mammoth Biosciences and HiFiBio. She reports research funding from Magenta Therapeutics, Tessera Therapeutics, Novartis, EMD-Serono, Gilead Pharmaceuticals, and Regeneron Pharmaceuticals. She reports consulting fees from Vertex. L.S.K. reports grants and personal fees from Bristol Myers Squibb. L.S.K.'s conflict-of-interest with Bristol Myers Squibb is managed under an agreement with Harvard Medical School. In addition, L.S.K. has a patent "WO2020172391A1: Methods and compositions relating to the treatment of GVHD" with royalties paid. I.M. has received research funding from Regeneron and Genentech, and he is a member of Garuda Therapeutics's scientific advisory board.

Data and materials availability:

All data associated with this study are in the paper or supplementary materials. Rhesus macaques microarray data are deposited in GEO (GSE accession number 228838). The DLL4-blocking antibodies REGN421 and REGN577 were manufactured by Regeneron and can be provided through a material transfer agreement (MTA). *Ccl19-Cre* transgenic and *Dll4*$^{f/f}$ mice were generated by Dr. Ludewig and Dr. Radtke, respectively, and are available through a MTA. All other reagents and data are available as described in the main text or supplementary material (data file S8 and S9).

References:

1. Hill GR, Betts BC, Tkachev V, Kean LS, Blazar BR, Current Concepts and Advances in Graft-Versus-Host Disease Immunology. Annu Rev Immunol, (2021).
2. Ara T et al. , Intestinal goblet cells protect against GVHD after allogeneic stem cell transplantation via Lypd8. Sci Transl Med 12, (2020).

3. Piper C et al. , Pathogenic Bhlhe40+ GM-CSF+ CD4+ T cells promote indirect alloantigen presentation in the GI tract during GVHD. Blood 135, 568–581 (2020). [PubMed: 31880771]
4. Koyama M et al. , MHC Class II Antigen Presentation by the Intestinal Epithelium Initiates Graft-versus-Host Disease and Is Influenced by the Microbiota. Immunity 51, 885–898 e887 (2019). [PubMed: 31542340]
5. Fu YY et al. , T Cell Recruitment to the Intestinal Stem Cell Compartment Drives Immune-Mediated Intestinal Damage after Allogeneic Transplantation. Immunity 51, 90–103 e103 (2019). [PubMed: 31278057]
6. Zhao D et al. , Survival signal REG3alpha prevents crypt apoptosis to control acute gastrointestinal graft-versus-host disease. J Clin Invest 128, 4970–4979 (2018). [PubMed: 30106382]
7. Mathewson ND et al. , Gut microbiome-derived metabolites modulate intestinal epithelial cell damage and mitigate graft-versus-host disease. Nat Immunol 17, 505–513 (2016). [PubMed: 26998764]
8. Hill GR, Ferrara JL, The primacy of the gastrointestinal tract as a target organ of acute graft-versus-host disease: rationale for the use of cytokine shields in allogeneic bone marrow transplantation. Blood 95, 2754–2759 (2000). [PubMed: 10779417]
9. Blazar BR, Hill GR, Murphy WJ, Dissecting the biology of allogeneic HSCT to enhance the GvT effect whilst minimizing GvHD. Nat Rev Clin Oncol 17, 475–492 (2020). [PubMed: 32313224]
10. Reddy P, Negrin R, Hill GR, Mouse models of bone marrow transplantation. Biol Blood Marrow Transplant 14, 129–135 (2008). [PubMed: 18162233]
11. Tkachev V et al. , Spatiotemporal single-cell profiling reveals that invasive and tissue-resident memory donor CD8(+) T cells drive gastrointestinal acute graft-versus-host disease. Sci Transl Med 13, (2021).
12. Watkins BK et al. , CD28 blockade controls T cell activation to prevent graft-versus-host disease in primates. J Clin Invest 128, 3991–4007 (2018). [PubMed: 30102255]
13. Tkachev V et al. , Combined OX40L and mTOR blockade controls effector T cell activation while preserving Treg reconstitution after transplant. Sci Transl Med 9, (2017).
14. Miller WP et al. , GVHD after haploidentical transplantation: a novel, MHC-defined rhesus macaque model identifies CD28− CD8+ T cells as a reservoir of breakthrough T-cell proliferation during costimulation blockade and sirolimus-based immunosuppression. Blood 116, 5403–5418 (2010). [PubMed: 20833977]
15. Furlan SN et al. , Transcriptome analysis of GVHD reveals aurora kinase A as a targetable pathway for disease prevention. Sci Transl Med 7, 315ra191 (2015).
16. Furlan SN et al. , Systems analysis uncovers inflammatory Th/Tc17-driven modules during acute GVHD in monkey and human T cells. Blood 128, 2568–2579 (2016). [PubMed: 27758873]
17. Radojcic V et al. , Notch signaling mediated by Delta-like ligands 1 and 4 controls the pathogenesis of chronic GVHD in mice. Blood 132, 2188–2200 (2018). [PubMed: 30181175]
18. Sandy AR et al. , T cell-specific notch inhibition blocks graft-versus-host disease by inducing a hyporesponsive program in alloreactive CD4+ and CD8+ T cells. J Immunol 190, 5818–5828 (2013). [PubMed: 23636056]
19. Zhang Y et al. , Notch signaling is a critical regulator of allogeneic CD4+ T-cell responses mediating graft-versus-host disease. Blood 117, 299–308 (2011). [PubMed: 20870902]
20. Chung J et al. , Early Notch Signals Induce a Pathogenic Molecular Signature during Priming of Alloantigen-Specific Conventional CD4(+) T Cells in Graft-versus-Host Disease. J Immunol 203, 557–568 (2019). [PubMed: 31182480]
21. Tran IT et al. , Blockade of individual Notch ligands and receptors controls graft-versus-host disease. J Clin Invest 123, 1590–1604 (2013). [PubMed: 23454750]
22. Kovall RA, Gebelein B, Sprinzak D, Kopan R, The Canonical Notch Signaling Pathway: Structural and Biochemical Insights into Shape, Sugar, and Force. Dev Cell 41, 228–241 (2017). [PubMed: 28486129]
23. Guruharsha KG, Kankel MW, Artavanis-Tsakonas S, The Notch signalling system: recent insights into the complexity of a conserved pathway. Nat Rev Genet 13, 654–666 (2012). [PubMed: 22868267]

24. Chung J et al. , Fibroblastic niches prime T cell alloimmunity through Delta-like Notch ligands. J Clin Invest 127, 1574–1588 (2017). [PubMed: 28319044]
25. Perkey E et al. , GCNT1-Mediated O-Glycosylation of the Sialomucin CD43 Is a Sensitive Indicator of Notch Signaling in Activated T Cells. J Immunol 204, 1674–1688 (2020). [PubMed: 32060138]
26. Mochizuki K et al. , Delta-like ligand 4 identifies a previously uncharacterized population of inflammatory dendritic cells that plays important roles in eliciting allogeneic T cell responses in mice. J Immunol 190, 3772–3782 (2013). [PubMed: 23440416]
27. VanDussen KL et al. , Notch signaling modulates proliferation and differentiation of intestinal crypt base columnar stem cells. Development 139, 488–497 (2012). [PubMed: 22190634]
28. van Es JH et al. , Notch/gamma-secretase inhibition turns proliferative cells in intestinal crypts and adenomas into goblet cells. Nature 435, 959–963 (2005). [PubMed: 15959515]
29. Deangelo DJ et al. , A phase I clinical trial of the notch inhibitor MK-0752 in patients with T-cell acute lymphoblastic leukemia/lymphoma (T-ALL) and other leukemias. Journal of Clinical Oncology 24, 6585–6585 (2006).
30. Wu Y et al. , Therapeutic antibody targeting of individual Notch receptors. Nature 464, 1052–1057 (2010). [PubMed: 20393564]
31. Watkins B et al. , Phase II Trial of Costimulation Blockade With Abatacept for Prevention of Acute GVHD. J Clin Oncol 39, 1865–1877 (2021). [PubMed: 33449816]
32. Chiorean EG et al. , A Phase I First-in-Human Study of Enoticumab (REGN421), a Fully Human Delta-like Ligand 4 (Dll4) Monoclonal Antibody in Patients with Advanced Solid Tumors. Clin Cancer Res 21, 2695–2703 (2015). [PubMed: 25724527]
33. Kuhnert F et al. , Dll4 Blockade in Stromal Cells Mediates Antitumor Effects in Preclinical Models of Ovarian Cancer. Cancer Res 75, 4086–4096 (2015). [PubMed: 26377940]
34. Schwabkey ZI, Jenq RR, Microbiome Anomalies in Allogeneic Hematopoietic Cell Transplantation. Annu Rev Med 71, 137–148 (2020). [PubMed: 31986084]
35. Pihusch M, Bleeding complications after hematopoietic stem cell transplantation. Semin Hematol 41, 93–100 (2004).
36. Petrovic A et al. , LPAM (alpha 4 beta 7 integrin) is an important homing integrin on alloreactive T cells in the development of intestinal graft-versus-host disease. Blood 103, 1542–1547 (2004). [PubMed: 14563643]
37. Sato T et al. , Role for CXCR6 in recruitment of activated CD8+ lymphocytes to inflamed liver. J Immunol 174, 277–283 (2005). [PubMed: 15611250]
38. Duffner U et al. , Role of CXCR3-induced donor T-cell migration in acute GVHD. Exp Hematol 31, 897–902 (2003). [PubMed: 14550805]
39. Moy RH et al. , Clinical and immunologic impact of CCR5 blockade in graft-versus-host disease prophylaxis. Blood 129, 906–916 (2017). [PubMed: 28057639]
40. Murai M et al. , Active participation of CCR5(+)CD8(+) T lymphocytes in the pathogenesis of liver injury in graft-versus-host disease. J Clin Invest 104, 49–57 (1999). [PubMed: 10393698]
41. de Almeida GP et al. , Human skin-resident host T cells can persist long term after allogeneic stem cell transplantation and maintain recirculation potential. Sci Immunol 7, eabe2634 (2022). [PubMed: 35089814]
42. Divito SJ et al. , Peripheral host T cells survive hematopoietic stem cell transplantation and promote graft-versus-host disease. J Clin Invest 130, 4624–4636 (2020). [PubMed: 32516138]
43. Chai Q et al. , Maturation of lymph node fibroblastic reticular cells from myofibroblastic precursors is critical for antiviral immunity. Immunity 38, 1013–1024 (2013). [PubMed: 23623380]
44. Zhou Y et al. , Metascape provides a biologist-oriented resource for the analysis of systems-level datasets. Nat Commun 10, 1523 (2019). [PubMed: 30944313]
45. DeNucci CC, Pagan AJ, Mitchell JS, Shimizu Y, Control of alpha4beta7 integrin expression and CD4 T cell homing by the beta1 integrin subunit. J Immunol 184, 2458–2467 (2010). [PubMed: 20118278]

46. Moreno-Layseca P, Icha J, Hamidi H, Ivaska J, Integrin trafficking in cells and tissues. Nat Cell Biol 21, 122–132 (2019). [PubMed: 30602723]
47. Mora JR et al. , Reciprocal and dynamic control of CD8 T cell homing by dendritic cells from skin- and gut-associated lymphoid tissues. J Exp Med 201, 303–316 (2005). [PubMed: 15642741]
48. Van de Walle I et al. , Specific Notch receptor-ligand interactions control human TCR-alphabeta/gammadelta development by inducing differential Notch signal strength. J Exp Med 210, 683–697 (2013). [PubMed: 23530123]
49. Dolens AC et al. , Distinct Notch1 and BCL11B requirements mediate human gammadelta/alphabeta T cell development. EMBO Rep 21, e49006 (2020). [PubMed: 32255245]
50. Zehn D, King C, Bevan MJ, Palmer E, TCR signaling requirements for activating T cells and for generating memory. Cell Mol Life Sci 69, 1565–1575 (2012). [PubMed: 22527712]
51. Shlomchik WD, Graft-versus-host disease. Nat Rev Immunol 7, 340–352 (2007). [PubMed: 17438575]
52. Waldman E et al. , Absence of beta7 integrin results in less graft-versus-host disease because of decreased homing of alloreactive T cells to intestine. Blood 107, 1703–1711 (2006). [PubMed: 16291587]
53. Berlin C et al. , Alpha 4 beta 7 integrin mediates lymphocyte binding to the mucosal vascular addressin MAdCAM-1. Cell 74, 185–195 (1993). [PubMed: 7687523]
54. Hamann A, Andrew DP, Jablonski-Westrich D, Holzmann B, Butcher EC, Role of alpha 4-integrins in lymphocyte homing to mucosal tissues in vivo. J Immunol 152, 3282–3293 (1994). [PubMed: 7511642]
55. Iwata M et al. , Retinoic acid imprints gut-homing specificity on T cells. Immunity 21, 527–538 (2004). [PubMed: 15485630]
56. Molenaar R et al. , Lymph node stromal cells support dendritic cell-induced gut-homing of T cells. J Immunol 183, 6395–6402 (2009). [PubMed: 19841174]
57. Danylesko I et al. , Anti-alpha4beta7 integrin monoclonal antibody (vedolizumab) for the treatment of steroid-resistant severe intestinal acute graft-versus-host disease. Bone Marrow Transplant 54, 987–993 (2019). [PubMed: 30356163]
58. Mehta RS et al. , Vedolizumab for Steroid Refractory Lower Gastrointestinal Tract Graft-Versus-Host Disease. Transplant Cell Ther 27, 272 e271–272 e275 (2021).
59. Pellegrinet L et al. , Dll1- and dll4-mediated notch signaling are required for homeostasis of intestinal stem cells. Gastroenterology 140, 1230–1240 e1231–1237 (2011). [PubMed: 21238454]
60. B. RL Russell WMS, The Principles of Humane Experimental Technique, (Methuen & Co Ltd., London, UK, 1959).
61. Tu L et al. , Notch signaling is an important regulator of type 2 immunity. J Exp Med 202, 1037–1042 (2005). [PubMed: 16230473]
62. Raghavan S, Bauer C, Mundschau G, Li Q, Fuchs E, Conditional ablation of beta1 integrin in skin. Severe defects in epidermal proliferation, basement membrane formation, and hair follicle invagination. J Cell Biol 150, 1149–1160 (2000). [PubMed: 10974002]
63. Irizarry RA et al. , Exploration, normalization, and summaries of high density oligonucleotide array probe level data. Biostatistics 4, 249–264 (2003). [PubMed: 12925520]
64. Johnson WE, Li C, Rabinovic A, Adjusting batch effects in microarray expression data using empirical Bayes methods. Biostatistics 8, 118–127 (2007). [PubMed: 16632515]
65. Bourgon R, Gentleman R, Huber W, Independent filtering increases detection power for high-throughput experiments. Proc Natl Acad Sci U S A 107, 9546–9551 (2010). [PubMed: 20460310]
66. Duan F, Pauley MA, Spindel ER, Zhang L, Norgren RB Jr., Large scale analysis of positional effects of single-base mismatches on microarray gene expression data. BioData Min 3, 2 (2010). [PubMed: 20429935]
67. Gentleman RC et al. , Bioconductor: open software development for computational biology and bioinformatics. Genome Biol 5, R80 (2004). [PubMed: 15461798]
68. Culhane AC, Thioulouse J, Perriere G, Higgins DG, MADE4: an R package for multivariate analysis of gene expression data. Bioinformatics 21, 2789–2790 (2005). [PubMed: 15797915]

69. Ritchie ME et al. , limma powers differential expression analyses for RNA-sequencing and microarray studies. Nucleic Acids Res 43, e47 (2015). [PubMed: 25605792]

70. Mootha VK et al. , PGC-1alpha-responsive genes involved in oxidative phosphorylation are coordinately downregulated in human diabetes. Nat Genet 34, 267–273 (2003). [PubMed: 12808457]

71. Subramanian A et al. , Gene set enrichment analysis: a knowledge-based approach for interpreting genome-wide expression profiles. Proc Natl Acad Sci U S A 102, 15545–15550 (2005). [PubMed: 16199517]

72. Shannon P et al. , Cytoscape: a software environment for integrated models of biomolecular interaction networks. Genome Res 13, 2498–2504 (2003). [PubMed: 14597658]

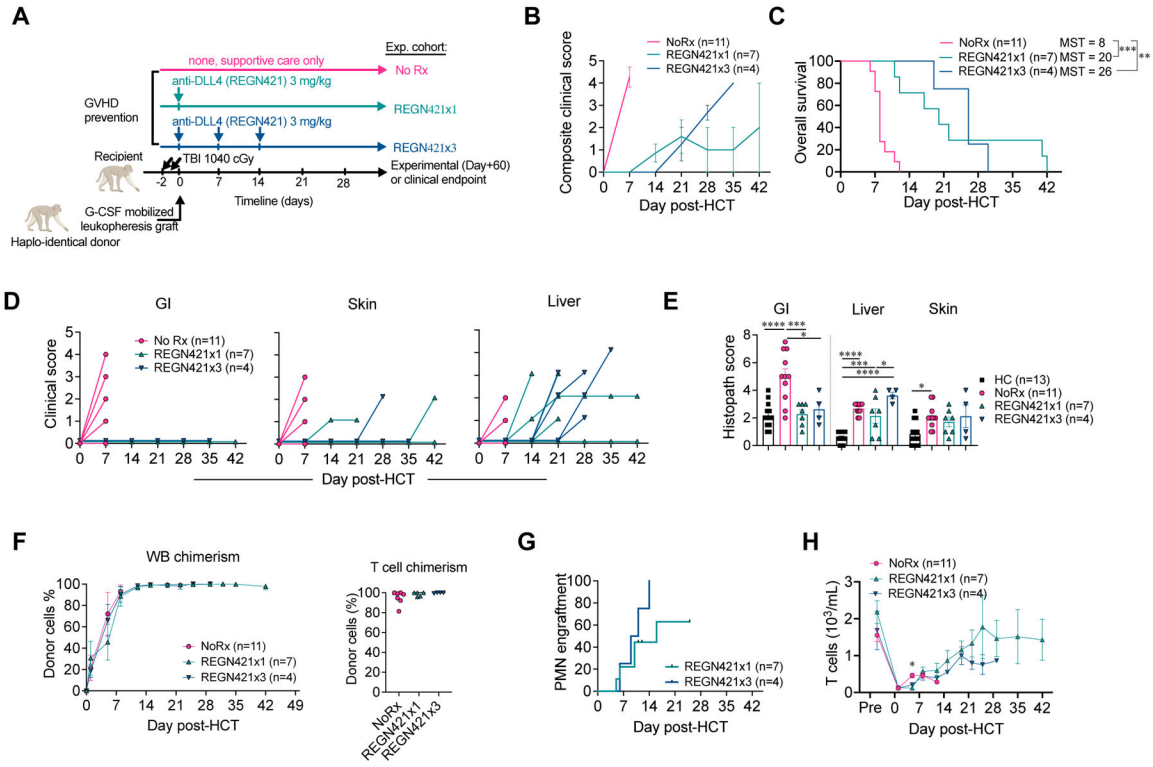

Figure 1. DLL4 blockade early after allo-HCT protects from GI-aGVHD in the NHP model.

(A) Experimental design, depicting major components of the NHP aGVHD model and dosing regimens with a single or three weekly doses of REGN421 (anti-DLL4). (B) Composite clinical score of allo-HCT recipients in NoRx, REGN421x1, and REGN421x3 cohorts. (C) Overall survival of allo-HCT recipients in the NoRx aGVHD cohort, REGN421x1, and REGN421x3 cohorts. Recipients euthanized based on pre-determined experimental endpoints were censored at terminal analysis. **p<0.01, ***p<0.001, log-rank (Mantel-Cox) test. (D) Clinical scores for GI, skin, and liver aGVHD in allo-HCT recipients, based on established criteria (diarrhea, skin rash and serum bilirubin) (14). (E) Histopathological aGVHD scores for skin, liver, and GI tract (terminal ileum and colon). *p<0.05, ***p<0.001, ****p<0.0001, ANOVA with Tukey post-hoc test. (F) Donor chimerism in whole blood (WB) and $CD3^{+}CD20^{-}$ T cells sorted at terminal analysis. (G) Polymorphonuclear neutrophil (PMN) engraftment in REGN421x1 and REGN421x3 cohorts. (H) Absolute number of T cells in peripheral blood.

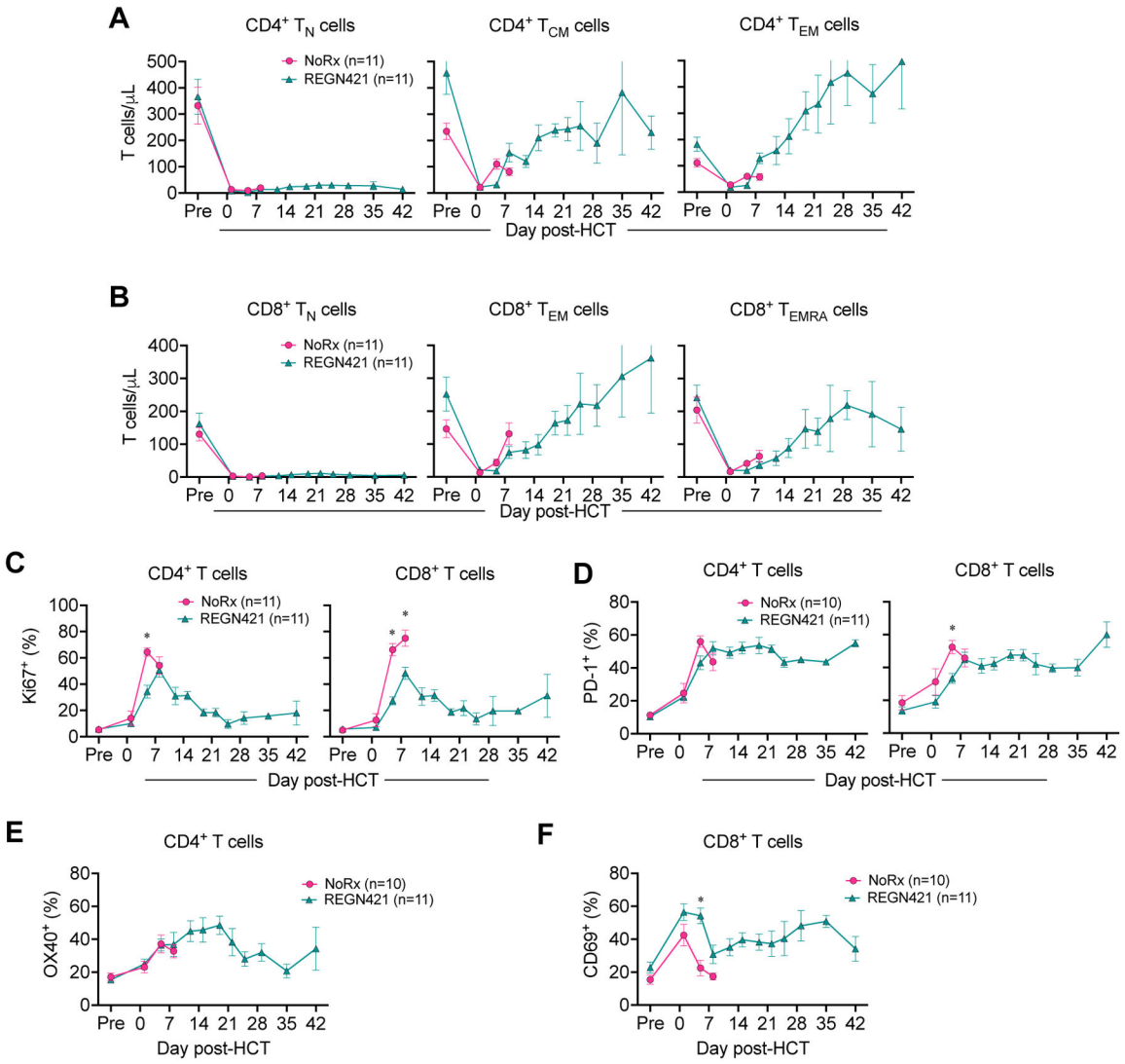

Figure 2. DLL4 blockade does not interfere with T cell differentiation and reconstitution following allo-HCT.

(A and B) Absolute number of $CD4^+$ (A) and $CD8^+$ (B) T cells with $CD45RA^+CCR7^+CD95^-$ naïve (T_N), $CD45RA^-CCR7^+$ central memory (T_{CM}), $CD45RA^-CCR7^-$ effector memory (T_{EM}) and $CD45RA^+CCR7^-$ terminal effector (T_{EMRA}) phenotypes in the blood of allo-HCT recipients. *p<0.05, Tukey-corrected t-test. (C and D) Relative number of $Ki67^+$ (C) or PD-1^+ (D) $CD4^+$ and $CD8^+$ T cells in the blood of allo-HCT recipients. *p<0.05, Tukey-corrected t-test. (E and F) Frequency of $OX40^+CD4^+$ (E) and $CD69^+CD8^+$ (F) T cells in the blood of allo-HCT recipients.

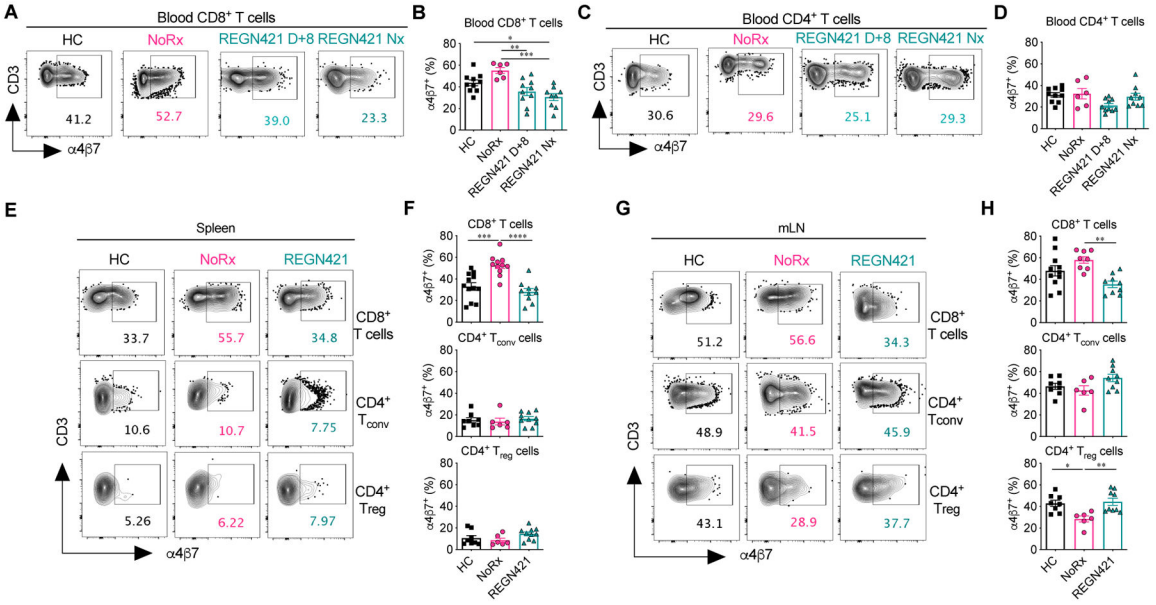

Figure 3. DLL4 blockade prevents T cell expression of the gut-homing α4β7 integrin during GVHD.

(A to D) Representative flow cytometry plots (A and C) and data (B and D) depicting the frequency of $\alpha4\beta7^{+}CD8^{+}$ (A and B) and $\alpha4\beta7^{+}CD4^{+}$ T cells (C and D) in the blood of healthy controls (HC; n=10) and allo-HCT recipients from the NoRx aGVHD (n=6) and REGN421 (n=10) cohorts. Data from the REGN421 cohort was collected at terminal analysis and day +8 (time-matched with the NoRx cohort). (E to H) Representative flow cytometry plots (E and G) and data (F and H) depicting the frequency of $\alpha4\beta7^{+}CD8^{+}$, $\alpha4\beta7^{+}CD4^{+}$ T_{conv} and $\alpha4\beta7^{+}CD4^{+}$ T_{reg} cells in spleen and mesenteric lymph nodes (mLN) of healthy controls (n=8 to 12 depending on the organ) versus allo-HCT recipients from the NoRx (n=8 to 11 depending on the organ) or REGN421 (n=10) experimental cohorts. For all plots: *p<0.05, **p<0.01, ***p<0.001, ***p<0.001, ****p<0.0001, one-way ANOVA with Tukey post-hoc test.

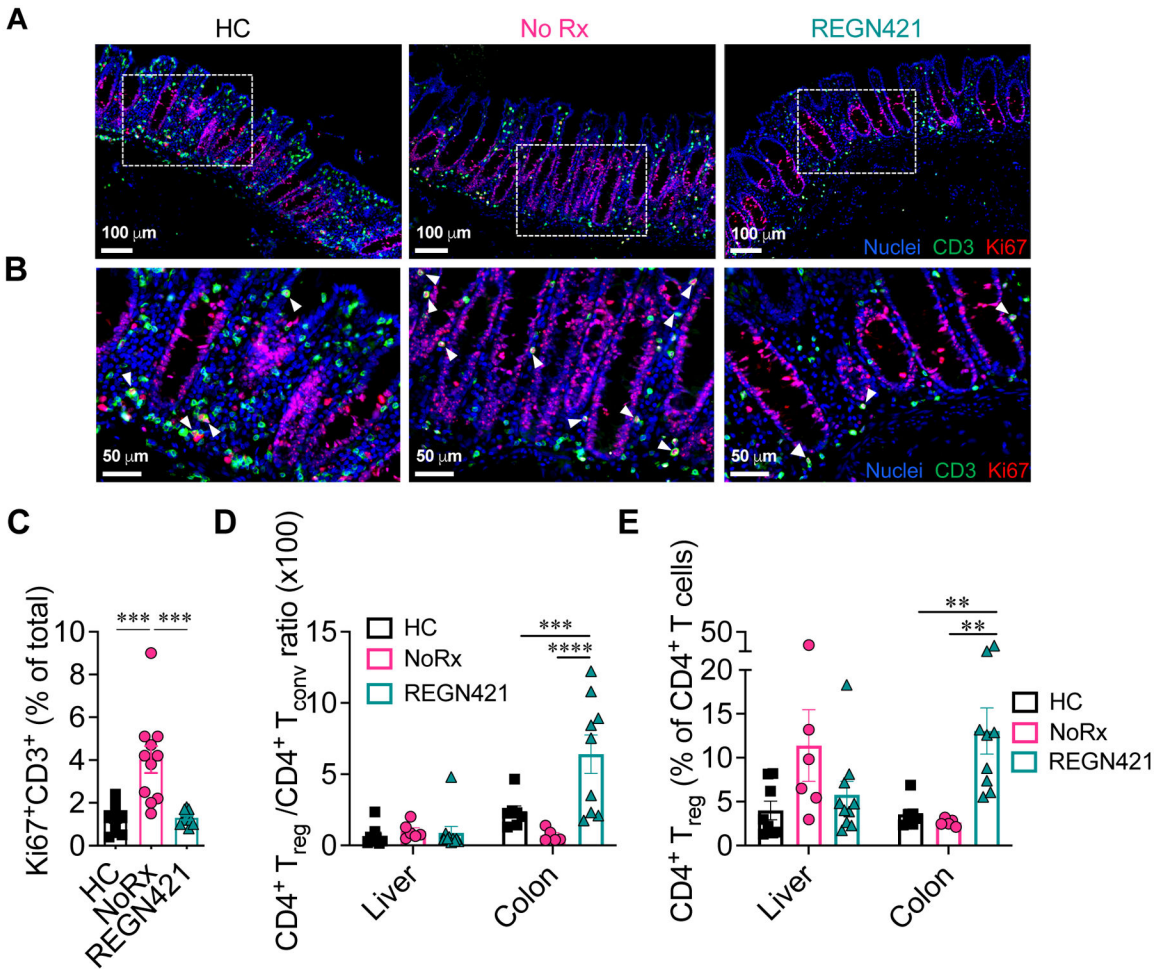

Figure 4. DLL4 blockade inhibits the accumulation of activated tissue-infiltrating T cells in the intestine during aGVHD.

(A to C) Immunofluorescence microcopy of paraffin-embedded colon collected at terminal analysis. Samples from healthy controls (HC) were compared to terminal analysis of allo-HCT recipients from untreated aGVHD (NoRx) or REGN421-treated experimental cohorts. (A) Representative staining for CD3 (green), Ki67 (red) and nuclei visualized by Hoechst (blue). (B) Cropped areas in (A) are enlarged with white arrowheads pointing to $CD3^+Ki67^+$ T cells. (C) Quantification of $Ki67^+CD3^+$ T cells among total nucleated cells (n=11 images from 5 animals per group). ***p<0.001, Kruskal-Wallis multiple comparison test. (D and E) T_{reg}:T_{conv} ratio (D) and %$Foxp3^+$ T_{reg} cells (E) were quantified among $CD4^+$ T cells in the liver and colon from healthy controls (n=8) versus at terminal analysis in allo-HCT recipients from untreated aGVHD (NoRx, n=7) or REGN421-treated (n=10) cohorts. **p<0.01, ***p<0.001, ****p<0.0001, one-way ANOVA with Tukey post-hoc test.

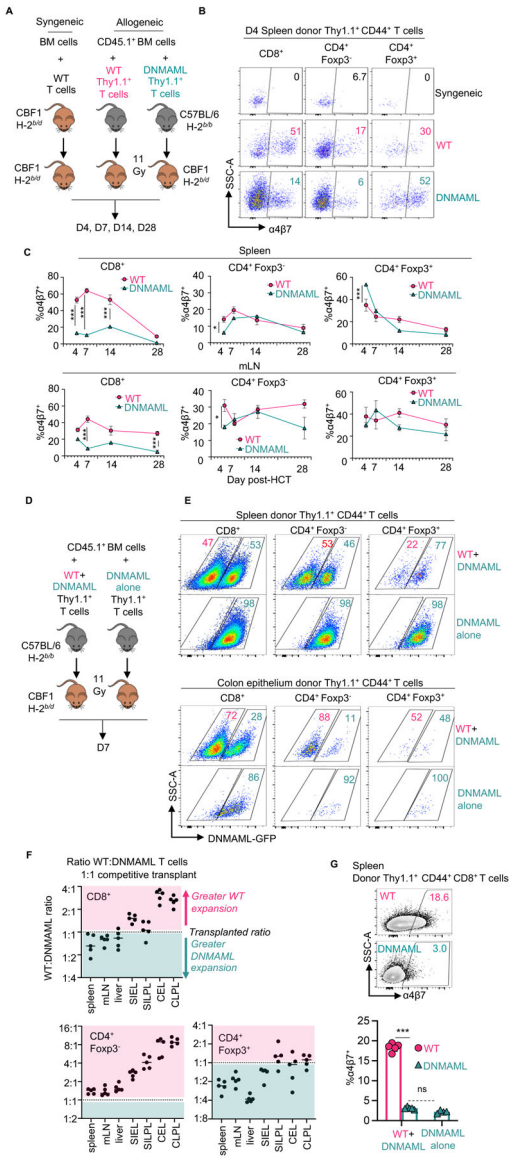

Figure 5. Cell-intrinsic canonical Notch signals control cell surface α4β7 and gut-homing potential in alloreactive T cells.

(A) 1×10^6 CBF1 syngeneic T cells (H-$2^{b/d}$), allogeneic wild-type B6-Thy1.1$^+$ T cells (H-$2^{b/b}$), or allogeneic Notch-deprived B6-DNMAML-Thy1.1$^+$ T cells (H-$2^{b/b}$) were transplanted into lethally irradiated CBF1 recipients (H-$2^{b/d}$) with CD45.1$^+$Thy1.2$^+$ T cell-depleted bone marrow (BM) to distinguish BM-derived cells from the T cell inoculum. (B and C) Representative flow cytometric analysis of α4β7 in donor-derived CD44$^+$CD8$^+$, Foxp3$^-$CD4$^+$ and Foxp3$^+$CD4$^+$ T cells in the spleen at day 4 (B) and summary data at indicated times post-transplant in spleen and mLN (C). n=3 mice per group and time point. (D) CBF1 recipients were transplanted as in (A), but with 1:1 wild type:DNMAML donor T cells or DNMAML T cells alone. (E) Representative flow cytometric plots showing relative accumulation of wild-type compared to DNMAML-GFP$^+$ T cells in spleen (top) versus colon epithelium (bottom) at day 7. (F) Organ-specific accumulation of wild-type to DNMAML T cells from the 1:1 competitive transplant was calculated for each T cell subset

and expressed as greater (pink) or less than (teal) the initial ratio. mLN, mesenteric lymph node; SIEL, small intestine epithelial lymphocytes; SILPL, small intestine lamina propria lymphocytes; CEL, colon epithelial lymphocytes; CLPL, colon lamina propria lymphocytes. (G) Representative flow cytometric analysis of $\alpha 4\beta 7$ in donor-derived $CD8^+$ T cells from inocula of wild-type and DNMAML T cells (1:1, left) versus DNMAML T cells alone. ns, not significant and ***$p<0.001$, one-way ANOVA with Tukey's post-hoc-test.

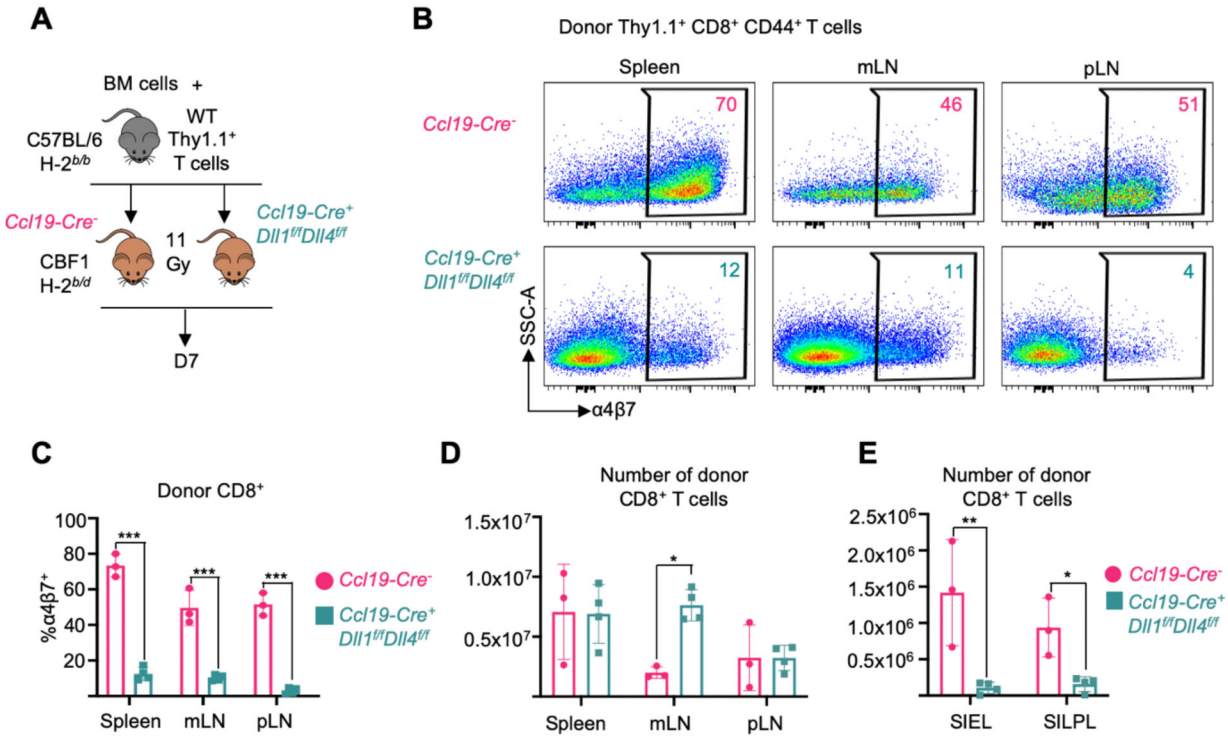

Figure 6. Secondary lymphoid organ *Ccl19-Cre*$^{+}$ fibroblastic reticular cells are critical sources of Delta-like Notch ligands.

(A) 1×10^{6} alloreactive T cells plus 1×10^{6} BM cells from C57BL/6 mice were transplanted into *Ccl19-Cre*$^{+}$ *Dll1*$^{f/f}$*Dll4*$^{f/f}$ or *Ccl19-Cre*^{neg} littermate control CBF1 mice after irradiation (11 Gy). Secondary lymphoid organs and small intestinal lymphocyte fractions were isolated at day 7 post-transplant. (B and C) Representative flow cytometry plots (B) and quantification (C) of α4β7 expression in donor Thy1.1^{+}CD44^{+}CD8^{+} T cells. SSC-A, side scatter area. (D and E) Absolute number of donor-derived CD8^{+} T cells in secondary lymphoid organs (D) and small intestinal lymphocyte fractions (E). n=3 or 4 mice per group. *p<0.05, **p<0.01, ***p<0.001, one-way ANOVA with Tukey's post-hoc tests. mLN, mesenteric lymph node; pLN, peripheral (cervical, axial, brachial, inguinal) lymph nodes; SIEL, small intestine epithelial lymphocytes; SILPL, small intestine lamina propria lymphocytes.

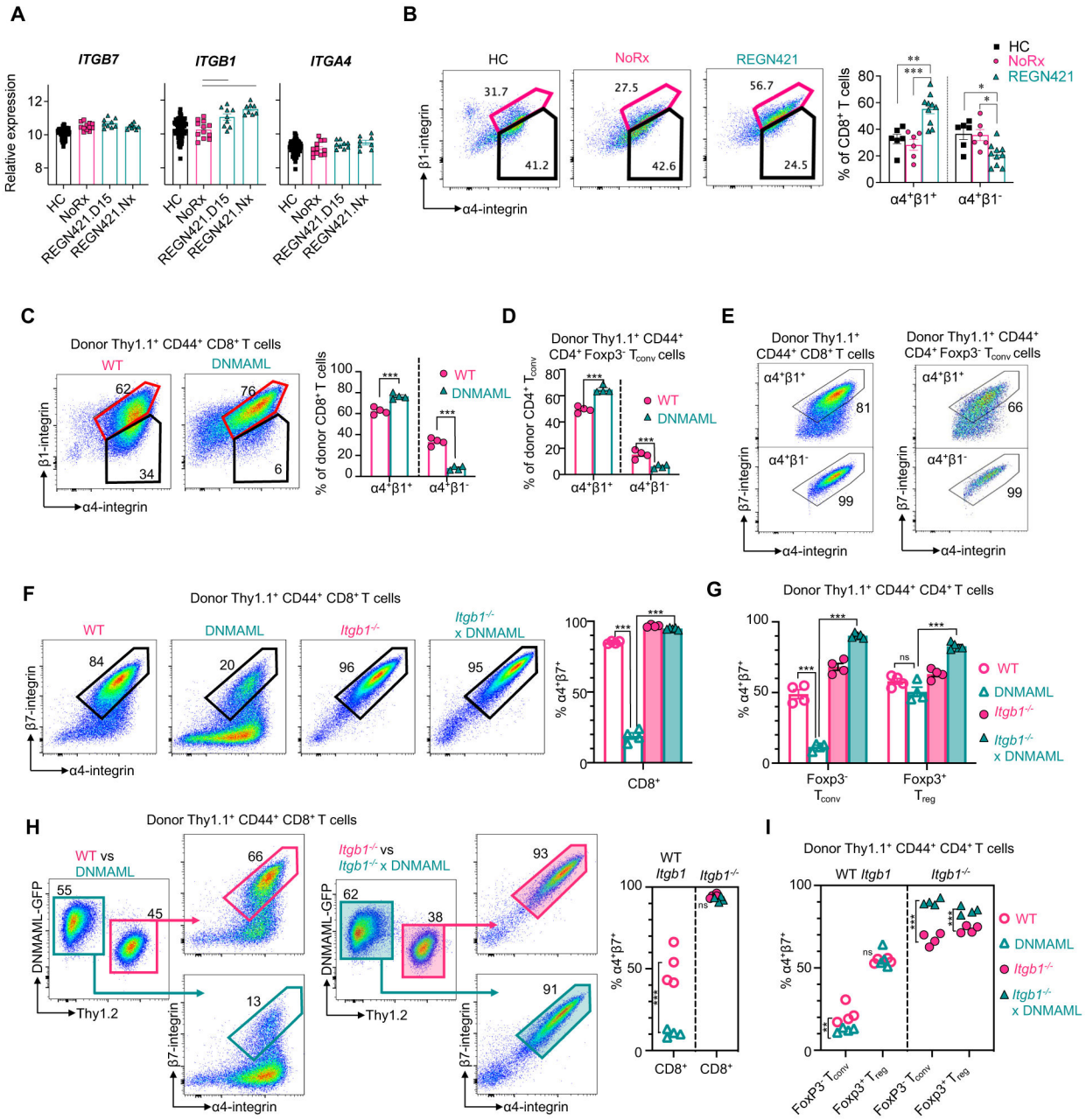

Figure 7. Notch signaling regulates α4β7 expression in alloreactive T cells through β1-integrin-dependent mechanisms.

(A) Relative abundance of *ITGA4*, *ITGB7* and *ITGB1* mRNA in T cells from healthy control NHP (HC), untreated allo-HCT recipients (NoRx) and allo-HCT recipients receiving anti-DLL4 antibodies (REGN421.D15: blood T cells at day 15; REGN421.Nx: blood T cells at necropsy). Lines indicate significant differences between cohorts ($p<0.05$, Benjamini-Hochberg correction). (B) Representative flow cytometry plots and summary data depicting the proportion of spleen $CD8^+$ T cells with cell surface α4 and β1 integrins, versus α4 without β1 in HC (n=6), NoRx aGVHD (n=6), and REGN421 (n=10) NHP cohorts. (C to G) 20×10^6 B6-Thy1.1$^+$ or B6-Thy1.1/1.2$^+$ splenocytes and lymph node cells from mice with

wild-type (WT), Notch-deprived (DNMAML), integrin β1-deficient (*Itgb1*$^{-/-}$) or Notch-deprived and β1-deficient (*Itgb1*$^{-/-}$ xDNMAML) T cells were transplanted into lethally irradiated CBF1 recipients (Thy1.2^{+}, H-2$^{b/d}$) with 1×10^{6} T cell-depleted B6-Thy1.2^{+} BM cells. (C and D) Representative flow cytometry plots and summary data for α4β1 (spleen, day 4.5) in donor-derived CD44^{+}CD8^{+} T cells (C) and CD44^{+}Foxp3^{-}CD4^{+} T$_{conv}$ cells (D). (E) Flow cytometry plots for α4β7 in α4^{+}β1^{+} (top) and α4^{+}β1^{-} (bottom) wild-type donor-derived spleen CD8^{+} (left) and CD4^{+} T$_{conv}$ cells (right). (F and G) Flow cytometry plots and summary data for α4β7 in donor-derived spleen CD8^{+} T cells (F), and summary data in donor-derived spleen CD4^{+} T$_{conv}$ cells and Foxp3^{+}CD4^{+} T$_{reg}$ cells (G). (H and I) CBF1 mice were transplanted as in (C to G), but with 15×10^{6}:15×10^{6} wild type:DNMAML T cells, or 15×10^{6}:15×10^{6} *Itgb1*$^{-/-}$:*Itgb1*$^{-/-}$ DNMAML T cells. (H) Flow cytometry plots showing α4β7 in wild-type versus DNMAML donor-derived spleen CD8^{+} T cells (left) and *Itgb1*$^{-/-}$ versus *Itgb1*$^{-/-}$ × DNMAML CD8^{+} T cells (right) with summary data (far right). (I) Cell surface α4β7 in donor-derived spleen CD4^{+} T$_{conv}$ and CD4^{+} T$_{reg}$ cells. n=4 mice per group. *p<0.05, **p<0.01, ***p<0.001; ns, not significant. Data were analyzed by a two-way ANOVA with Tukey's post-hoc-test.